Available online at www.sciencedirect.com

ScienceDirect

IFAC Papers Online CONFERENCE PAPER ARCHIVE

IFAC-PapersOnLine 48-12 (2015) 468–473

Optimized connected cruise control with time delay

Jin I. Ge and Gábor Orosz

Department of Mechanical Engineering, University of Michigan, Ann Arbor, MI 48109, USA (e-mail: gejin@umich.edu, orosz@umich.edu).

Abstract: In this paper, we optimize the connectivity structure for connected cruise control (CCC) using linear quadratic regulation (LQR) while taking into account driver reaction time delay. We consider that a CCC-equipped vehicle receives position and velocity signals through wireless vehicle-to-vehicle (V2V) communication from multiple vehicles ahead and minimize a cost function defined by headway and velocity errors and the acceleration of the CCC vehicle over an infinite horizon. The resulting optimal feedback contains distributed delay. We show that the feedback gains and the distribution kernels can be obtained recursively as signals from vehicles farther ahead become available. Moreover, the gains exhibit exponential decay as the number of cars between the source and the CCC vehicle increases. The performance of the developed CCC controller is verified by numerical simulations.

Keywords: Connected cruise control, Optimization, Connectivity structure, Time delay

1. INTRODUCTION

Connected cruise control (CCC) can be used to maintain smooth traffic flow by exploiting wireless vehicle-to-vehicle (V2V) communication; see Ge and Orosz (2014a), Zhang and Orosz (2015), Orosz (2014), Qin et al. (2014). The CCC controller receives information about the motion of multiple vehicles ahead and assists the human driver or actuates the vehicle based on these signals. Including every available signal in the feedback loop requires one to tune a large number of gains. Thus, it is necessary to optimize the connectivity structure, that is, to weigh the available motion information in order to determine feedback gains systematically. Ploeg et al. (2014) and Wang et al. (2014) discussed optimization of vehicle platoons with small numbers of cars. Ge and Orosz (2014b) discussed optimization of connectivity structure in a general scenario where a CCC vehicle receives V2V signals from n preceding vehicles that are driven by human drivers. However, in these works driver reaction time delay was omitted, which may significantly influence the dynamics of vehicle strings; see Orosz et al. (2010), Ge and Orosz (2014a), Zhang and Orosz (2015).

In this paper we assume that non-CCC vehicles are human driven, and their driver reaction time is modeled as a discrete time delay in the range of $0.4 - 1$ [s]. We assume drivers with identical parameters, but the proposed control design can also be implemented for non-identical parameters. We assume that the CCC vehicle receives position and velocity signals from n non-CCC vehicles ahead (Fig. 1(a)), and formulate the optimization problem using linear quadratic regulation (LQR), where the headway and velocity fluctuations and the acceleration of the CCC vehicle are penalized. The obtained control law is both necessary and sufficient for optimality. We show that the gains of the optimized controller follow the spatial causality of traffic systems: information from vehicles farther downstream has less influence on the CCC vehicle and including motion information from vehicles farther ahead does not change the feedback laws concerning the signals from closer vehicles. The optimal gains are determined in terms of the weighting factors used in the optimization and the driver parameters of the non-CCC vehicles.

2. CONNECTED CRUISE CONTROL

We consider a string of $n+1$ vehicles traveling on a single lane as shown in Fig. 1(a) where the vehicle at the tail implements a connected cruise control algorithm using position and velocity signals of n preceding vehicles. The longitudinal dynamics of the CCC vehicle is given by

$$\begin{aligned} \dot{h}_1(t) &= v_2(t) - v_1(t)\,, \\ \dot{v}_1(t) &= u(t)\,, \end{aligned} \tag{1}$$

where the dot stands for differentiation with respect to time t, h_1 is the headway (i.e., the bumper-to-bumper distance between the CCC vehicle and the vehicle immediately ahead), and v_1 is the velocity of the CCC vehicle; see Fig. 1(a). Finally, $u(t)$ is the control input that will be designed using LQR based on the position and velocity of other vehicles.

For the dynamics of non-CCC vehicles, we ignore the driveline and engine dynamics, and use the car-following model

$$\begin{aligned} \dot{h}_i(t) &= v_{i+1}(t) - v_i(t)\,, \\ \dot{v}_i(t) &= \alpha\big(V(h_i(t-\tau)) - v_i(t-\tau)\big) \\ &\quad + \beta\big(v_{i+1}(t-\tau) - v_i(t-\tau)\big)\,, \end{aligned} \tag{2}$$

for $i = 2, \ldots, n$, where h_i and v_i denote the headway and velocity of the i-th vehicle; see Fig. 1(a). The gain α is for the difference between the desired velocity and the actual velocity of the vehicle, while the gain β is for the

10.1016/j.ifacol.2015.09.423

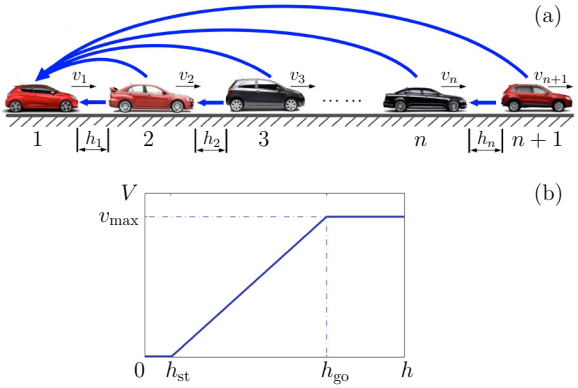

Fig. 1. (a): A string of $n+1$ vehicles with a CCC vehicle at the tail receiving signals from multiple vehicles via V2V communication. (b): The range policy (3).

velocity difference between the vehicle and its immediate predecessor. Model (2) considers identical vehicles, but the method proposed here is applicable when considering non-identical gains α_i, β_i and delays τ_i, $i = 2, \ldots, n$.

The desired velocity is determined by the headway using the range policy

$$V(h) = \begin{cases} 0\,, & h \le h_{\rm st}\,, \\ v_{\max}\,\dfrac{h - h_{\rm st}}{h_{\rm go} - h_{\rm st}}\,, & h_{\rm st} < h < h_{\rm go}\,, \\ v_{\max}\,, & h \ge h_{\rm go}\,, \end{cases} \tag{3}$$

shown in Fig. 1 (b). That is, the desired velocity is zero for small headways ($h \le h_{\rm st}$) and equal to the maximum speed $v_{\max}$ for large headways ($h \ge h_{\rm go}$). Between these, the desired velocity increases with the headway linearly. Here, we consider $v_{\max} = 30$ [m/s], $h_{\rm st} = 5$ [m], $h_{\rm go} = 35$ [m] that corresponds to realistic traffic data. Many other range policies may be chosen, but the qualitative dynamics remain similar if the above characteristics are considered; see Orosz et al. (2010).

3. CCC DESIGN USING LQR

In this section, we formulate the CCC design as a linear quadratic regulator (LQR) with delay. Since the CCC vehicle tries to maintain constant velocity and headway without using large acceleration/deceleration, we minimize a cost function containing its headway and velocity fluctuations and its acceleration. The solution gives the gains for the CCC vehicle with respect to the current and delayed headways and velocities of the vehicles ahead.

The dynamics of the connected vehicle system (1,2) is assumed to be in the vicinity of equilibrium where all vehicles travel with the same constant velocity and maintain constant headway, that is,

$$h_i(t) \equiv h^*\,, \quad v_i(t) \equiv v^* = V(h^*)\,, \tag{4}$$

for $i = 1, \ldots, n+1$. Here the equilibrium velocity v^* is determined by the head vehicle, while the equilibrium headway h^* can be calculated from the range policy (3).

We define the headway perturbations $\tilde h_i(t) = h_i(t) - h^*$ and velocity perturbations $\tilde v_i(t) = v_i(t) - v^*$, $i = 1, \ldots, n+1$, and linearize (1,2) about the equilibrium (4), yielding the delay differential equation (DDE)

$$\begin{aligned} \dot{\tilde h}_1(t) &= \tilde v_2(t) - \tilde v_1(t)\,, \\ \dot{\tilde v}_1(t) &= u(t)\,, \\ \dot{\tilde h}_i(t) &= \tilde v_{i+1}(t) - \tilde v_i(t)\,, \\ \dot{\tilde v}_i(t) &= \alpha\big(f^* \tilde h_i(t-\tau) - \tilde v_i(t-\tau)\big) \\ &\quad + \beta\left(\tilde v_{i+1}(t-\tau) - \tilde v_i(t-\tau)\right), \end{aligned} \tag{5}$$

for $i = 2, \ldots, n$. Here $f^* = V'(h^*)$ is the derivative of the range policy (3) at the equilibrium and for $h \in (h_{\rm st}, h_{\rm go})$ the corresponding time headway is $t_{\rm h} = 1/f^*$. Here $f^* = 1$ [1/s], yielding the time headway $t_{\rm h} = 1$ [s] (cf. (3)).

Let us define the vector $X = [x_1^{\rm T}, \ldots, x_n^{\rm T}]^{\rm T}$, where $x_i = [\tilde h_i, \tilde v_i]^{\rm T}$, and rewrite the system (5) as

$$\dot X(t) = \mathbf{A}X(t) + \mathbf{B}X(t-\tau) + \mathbf{D}u(t) + \phi(t)\,, \tag{6}$$

where $\phi(t) = [0, \ldots, 0, \tilde v_{n+1}(t), \beta \tilde v_{n+1}(t-\tau)]^{\rm T}$ denotes the disturbance and the coefficient matrices are given by

$$\mathbf{A} = \begin{bmatrix} \mathbf{A}_0 & \mathbf{A}_1 & & \\ & \mathbf{A}_0 & \mathbf{A}_1 & \\ & & \ddots & \ddots \\ & & & \mathbf{A}_0 \end{bmatrix}, \ \mathbf{B} = \begin{bmatrix} \mathbf{0} & \mathbf{0} & & \\ & \mathbf{B}_0 & \mathbf{B}_1 & \\ & & \ddots & \ddots \\ & & & \mathbf{B}_0 \end{bmatrix}, \ \mathbf{D} = \begin{bmatrix} \mathbf{D}_1 \\ \mathbf{0} \\ \vdots \\ \mathbf{0} \end{bmatrix}, \tag{7}$$

with block matrices

$$\begin{aligned} \mathbf{A}_0 &= \begin{bmatrix} 0 & -1 \\ 0 & 0 \end{bmatrix}, & \mathbf{A}_1 &= \begin{bmatrix} 0 & 1 \\ 0 & 0 \end{bmatrix}, \\ \mathbf{B}_0 &= \begin{bmatrix} 0 & 0 \\ \alpha f^* & -\alpha - \beta \end{bmatrix}, & \mathbf{B}_1 &= \begin{bmatrix} 0 & 0 \\ 0 & \beta \end{bmatrix}, \quad \mathbf{D}_1 = \begin{bmatrix} 0 \\ 1 \end{bmatrix}. \end{aligned} \tag{8}$$

Note that $\mathbf{A}$, $\mathbf{B}$ are upper-triangular because vehicles only react to the motion of vehicles ahead (except in emergency situations that are not considered here). We assume the non-CCC vehicles are plant stable, i.e., they are able to maintain the uniform flow (4) when the vehicles ahead travel with constant speed v^*; see Orosz (2014). Then (6,7) is stabilizable, and we define cost function

$$J_{t_{\rm f}}(u, X) = \int_0^{t_{\rm f}} \Big(u^2(t) + X^{\rm T}(t) \mathbf{\Gamma} X(t)\Big) {\rm d}t\,, \tag{9}$$

where the first term corresponds to the magnitude of the CCC vehicle's acceleration with weighting factor set to 1. The second term corresponds to the fluctuation of vehicles' headway and velocity around the uniform traffic flow $X(t) \equiv 0$ with weighting factor

$$\mathbf{\Gamma} = {\rm diag}[\gamma_1, \gamma_2, \ldots, \gamma_{2n-1}, \gamma_{2n}] \in \mathbb{R}^{2n \times 2n}, \tag{10}$$

where γ_{2k-1} and γ_{2k} are the weights for the headway and velocity errors of the $k^{\rm th}$ vehicle. Since only the CCC vehicle is controlled, the choice of γ_{2k-1} and γ_{2k}, $k = 2, \ldots, n$ does not influence the optimal control input, so we set these coefficients to zero.

We define the augmented state $Y(t) = [X^{\rm T}(t)\, 1]^{\rm T}$ to place the disturbance term $\phi(t)$ in (6) into a time-variant coefficient matrix. We also rescale the time using the driver reaction time τ, i.e., $\hat t = t/\tau$, $\hat t_{\rm f} = t_{\rm f}/\tau$. By abuse of notation, we drop the hat immediately and obtain

$$\dot Y(t) = \tilde{\mathbf{A}}(t) Y(t) + \tilde{\mathbf{B}} Y(t-1) + \tilde{\mathbf{D}} u(t)\,, \tag{11}$$

where the dot denotes the derivative with respect to the rescaled time and

$$\tilde{\mathbf{A}}(t) = \begin{bmatrix} \tau\mathbf{A} & \tau\phi(t) \\ 0 & 0 \end{bmatrix}, \quad \tilde{\mathbf{B}} = \begin{bmatrix} \tau\mathbf{B} & 0 \\ 0 & 0 \end{bmatrix}, \quad \tilde{\mathbf{D}} = \begin{bmatrix} \tau\mathbf{D} \\ 0 \end{bmatrix}. \tag{12}$$

The cost function (9) can be rewritten accordingly

$$J_{t_\mathrm{f}}(u,Y)=\int_0^{t_\mathrm{f}}\Big(u^2(t)+Y^\mathrm{T}(t)\tilde{\mathbf{\Gamma}}Y(t)\Big)\,\mathrm{d}t\,, \tag{13}$$

where $\tilde{\mathbf{\Gamma}}=\begin{bmatrix}\mathbf{\Gamma} & 0\\ 0 & 0\end{bmatrix}$.

The optimal control input of (11,13) is given by

$$u(t)=-\tilde{\mathbf{D}}^\mathrm{T}\bigg(\mathbf{P}(t)Y(t)+\int_{-1}^{0}\mathbf{Q}(t,\theta)Y(t+\theta)\mathrm{d}\theta\bigg)\,, \tag{14}$$

see Kolmanovskii and Myshkis (1992), where the matrices $\mathbf{P}(t)$ and $\mathbf{Q}(t,\theta)$ are obtained by solving the partial differential equation (PDE)

$$\begin{aligned}
-\dot{\mathbf{P}}(t)&=\tilde{\mathbf{A}}^\mathrm{T}\mathbf{P}(t)+\mathbf{P}(t)\tilde{\mathbf{A}}-\mathbf{P}(t)\tilde{\mathbf{D}}\tilde{\mathbf{D}}^\mathrm{T}\mathbf{P}(t)+\tilde{\mathbf{\Gamma}}\\
&\quad+\mathbf{Q}(t,0)+\mathbf{Q}^\mathrm{T}(t,0)\,,\\
(\partial_\theta-\partial_t)\mathbf{Q}(t,\theta)&=\big(\tilde{\mathbf{A}}^\mathrm{T}-\mathbf{P}\tilde{\mathbf{D}}\tilde{\mathbf{D}}^\mathrm{T}\big)\mathbf{Q}(t,\theta)+\mathbf{R}(t,0,\theta)\,,\\
(\partial_\xi+\partial_\theta-\partial_t)\mathbf{R}(t,\xi,\theta)&=-\mathbf{Q}^\mathrm{T}(t,\xi)\tilde{\mathbf{D}}\tilde{\mathbf{D}}^\mathrm{T}\mathbf{Q}(t,\theta)\,,
\end{aligned} \tag{15}$$

with boundary conditions

$$\begin{aligned}
&\mathbf{P}(t_\mathrm{f})=\mathbf{0}\,,\\
&\mathbf{Q}(t_\mathrm{f},\theta)=\mathbf{0}\,,\qquad \mathbf{Q}(t,-1)=\mathbf{P}^\mathrm{T}\tilde{\mathbf{B}}\,,\\
&\mathbf{R}(t_\mathrm{f},\xi,\theta)=\mathbf{0}\,,\quad \mathbf{R}(t,-1,\theta)=\tilde{\mathbf{B}}^\mathrm{T}\mathbf{Q}(t,\theta)\,,
\end{aligned} \tag{16}$$

where $\mathbf{P}(t)$ is symmetric and $\mathbf{R}^\mathrm{T}(t,\xi,\theta)=\mathbf{R}(t,\theta,\xi)$. Given the structure of coefficient matrices (12), the matrices $\mathbf{P}(t)$, $\mathbf{Q}(t,\theta)$ and $\mathbf{R}(t,\xi,\theta)$ can be constructed as

$$\mathbf{P}=\begin{bmatrix}\mathbf{P}_1 & \mathbf{P}_2\\ \mathbf{P}_3 & \mathbf{P}_4\end{bmatrix},\quad \mathbf{Q}=\begin{bmatrix}\mathbf{Q}_1 & \mathbf{Q}_2\\ \mathbf{Q}_3 & \mathbf{Q}_4\end{bmatrix},\quad \mathbf{R}=\begin{bmatrix}\mathbf{R}_1 & \mathbf{R}_2\\ \mathbf{R}_3 & \mathbf{R}_4\end{bmatrix}, \tag{17}$$

where $\mathbf{P}_1,\mathbf{Q}_1,\mathbf{R}_1\in\mathbb{R}^{2n\times 2n}$, $\mathbf{P}_2,\mathbf{Q}_2,\mathbf{R}_2\in\mathbb{R}^{2n\times 1}$, $\mathbf{P}_3,\mathbf{Q}_3,\mathbf{R}_3\in\mathbb{R}^{1\times 2n}$, and $\mathbf{P}_4,\mathbf{Q}_4,\mathbf{R}_4$ are scalars. Recall that $\mathbf{P}(t)$ is symmetric, and thus, $\mathbf{P}_1(t)=\mathbf{P}_1^\mathrm{T}(t)$, $\mathbf{P}_2(t)=\mathbf{P}_3^\mathrm{T}(t)$. Moreover, $\mathbf{R}(t,\xi,\theta)=\mathbf{R}^\mathrm{T}(t,\theta,\xi)$ yields $\mathbf{R}_1(t,\xi,\theta)=\mathbf{R}_1^\mathrm{T}(t,\theta,\xi)$, $\mathbf{R}_2(t,\xi,\theta)=\mathbf{R}_3^\mathrm{T}(t,\theta,\xi)$.

Thus, the optimal controller (14) becomes

$$\begin{aligned}
u(t)=-\tau\mathbf{D}^\mathrm{T}\bigg(&\mathbf{P}_1(t)X(t)+\int_{-1}^{0}\mathbf{Q}_1(t,\theta)X(t+\theta)\mathrm{d}\theta\\
&+\mathbf{P}_2(t)+\int_{-1}^{0}\mathbf{Q}_2(t,\theta)\mathrm{d}\theta\bigg)\,.
\end{aligned} \tag{18}$$

In Appendix A we substitute (17) into (15,16) and discuss the solution in detail; see (A.1,A.3,A.5,A.7). While (18) gives a general solution to the finite-horizon delayed optimization problem with disturbance, it cannot be implemented in real time since the disturbance $\phi(t)$ is unknown a priori. Here we ignore the disturbance $\phi(t)$ (that is, ignore $\tilde{v}_{n+1}(t)$) by considering

$$\mathbf{P}_2(t)\equiv\mathbf{0}\,,\qquad \mathbf{Q}_2(t,\theta)\equiv\mathbf{0}\,. \tag{19}$$

This simplification does not influence the stability of the multi-vehicle system, and we will discuss the effects of disturbance briefly in Section 3.3.

Since $\mathbf{P}_1(t),\mathbf{Q}_1(t,\theta),\mathbf{R}_1(t,\xi,\theta)$ are given by (A.1), which is an initial value problem backwards in time, we consider the steady-state solution in t:

$$\mathbf{P}_1(t)\equiv\mathbf{P}_1,\quad \mathbf{Q}_1(t,\theta)\equiv\mathbf{Q}_1(\theta),\quad \mathbf{R}_1(t,\xi,\theta)\equiv\mathbf{R}_1(\xi,\theta), \tag{20}$$

which is equivalent to setting time horizon $t_\mathrm{f}\to\infty$ in the cost function (9).

Thus (19) and (20) lead to the simplified controller

$$u(t)=-\tau\mathbf{D}^\mathrm{T}\bigg(\mathbf{P}_1X(t)+\int_{-1}^{0}\mathbf{Q}_1(\theta)X(t+\theta)\mathrm{d}\theta\bigg)\,, \tag{21}$$

cf. (18), where the matrices $\mathbf{P}_1$, $\mathbf{Q}_1(\theta)$ are given by

$$\begin{aligned}
&\tau\mathbf{A}^\mathrm{T}\mathbf{P}_1+\tau\mathbf{P}_1\mathbf{A}-\tau^2\mathbf{P}_1\mathbf{D}\mathbf{D}^\mathrm{T}\mathbf{P}_1+\mathbf{Q}_1(0)+\mathbf{Q}_1^\mathrm{T}(0)=-\mathbf{\Gamma}\,,\\
&\partial_\theta\mathbf{Q}_1(\theta)=\big(\tau\mathbf{A}^\mathrm{T}-\tau^2\mathbf{P}_1\mathbf{D}\mathbf{D}^\mathrm{T}\big)\mathbf{Q}_1(\theta)+\mathbf{R}_1(0,\theta)\,,\\
&(\partial_\xi+\partial_\theta)\mathbf{R}_1(\xi,\theta)=-\tau^2\mathbf{Q}_1^\mathrm{T}(\xi)\mathbf{D}\mathbf{D}^\mathrm{T}\mathbf{Q}_1(\theta)\,,
\end{aligned} \tag{22}$$

with boundary conditions

$$\mathbf{Q}_1(-1)=\tau\mathbf{P}_1\mathbf{B}\,,\qquad \mathbf{R}_1(-1,\theta)=\tau\mathbf{B}^\mathrm{T}\mathbf{Q}_1(\theta)\,, \tag{23}$$

which can be attained by setting $t_\mathrm{f}\to\infty$ in (A.1,A.2).

3.1 Decomposition of the solution

The numerical solution of (22,23) with general $\mathbf{A},\mathbf{B},\mathbf{D}$ matrices is given in Ross and Flugge-Lotz (1969). Here we take advantage of the upper-triangular block structure of $\mathbf{A},\mathbf{B}$ in order to obtain an analytical solution. Since only the second row in $\mathbf{D}$ is non-zero, cf. (7,8), only the second rows of $\mathbf{P}_1,\mathbf{Q}_1(\theta)$ appear in the controller (21). We introduce the notation

$$\mathbf{P}_1=\begin{bmatrix}\mathbf{P}_{11} & \cdots & \mathbf{P}_{1n}\\ \vdots & \ddots & \vdots\\ \mathbf{P}_{n1} & \cdots & \mathbf{P}_{nn}\end{bmatrix},\quad \mathbf{Q}_1(\theta)=\begin{bmatrix}\mathbf{Q}_{11}(\theta) & \cdots & \mathbf{Q}_{1n}(\theta)\\ \vdots & \ddots & \vdots\\ \mathbf{Q}_{n1}(\theta) & \cdots & \mathbf{Q}_{nn}(\theta)\end{bmatrix}, \tag{24}$$

where $\mathbf{P}_{ji},\mathbf{Q}_{ji}(\theta)\in\mathbb{R}^{2\times 2}$, $i,j=1,\dots,n$, and rewrite (21) as

$$u(t)=-\tau\mathbf{D}_1^\mathrm{T}\sum_{i=1}^{n}\bigg(\mathbf{P}_{1i}x_i(t)+\int_{-1}^{0}\mathbf{Q}_{1i}(\theta)x_i(t+\theta)\mathrm{d}\theta\bigg)\,, \tag{25}$$

where $x_i=[\tilde{h}_i,\tilde{v}_i]^\mathrm{T}$. This shows that we only need to derive $\mathbf{P}_{1i},\mathbf{Q}_{1i}(\theta)$, $i=1,\dots,n$ to construct the controller. Substituting (24) into (22,23), we obtain equations for each block $\mathbf{P}_{ij},\mathbf{Q}_{ij}(\theta),\mathbf{R}_{ij}(\xi,\theta)$, $i,j=1,\dots,n$, which can be solved recursively. Specifically, $\mathbf{P}_{11}$ and $\mathbf{Q}_{11}(\theta)$ are given by

$$\begin{aligned}
&\tau\hat{\mathbf{A}}_0^\mathrm{T}\mathbf{P}_{11}+\tau\mathbf{P}_{11}\mathbf{A}_0+\mathbf{Q}_{11}(0)+\mathbf{Q}_{11}^\mathrm{T}(0)+\mathrm{diag}[\gamma_1,\gamma_2]=\mathbf{0}\,,\\
&\partial_\theta\mathbf{Q}_{11}(\theta)=\hat{\mathbf{A}}_0\mathbf{Q}_{11}(\theta)+\mathbf{R}_{11}(0,\theta)\,,\\
&(\partial_\xi+\partial_\theta)\mathbf{R}_{11}(\xi,\theta)=-\tau^2\mathbf{Q}_{11}^\mathrm{T}(\xi)\mathbf{D}\mathbf{D}^\mathrm{T}\mathbf{Q}_{11}(\theta)\,,
\end{aligned} \tag{26}$$

with boundary conditions

$$\mathbf{Q}_{11}(-1)=\mathbf{0}\,,\qquad \mathbf{R}_{11}(-1,\theta)=\mathbf{0}\,, \tag{27}$$

where

$$\hat{\mathbf{A}}_0=\tau\mathbf{A}_0^\mathrm{T}-\tau^2\mathbf{P}_{11}\mathbf{D}_1\mathbf{D}_1^\mathrm{T}\,. \tag{28}$$

The solution of (26,27) is given by

$$\begin{aligned}
\mathbf{P}_{11}&=\frac{1}{\tau}\begin{bmatrix}\sqrt{\gamma_1(\gamma_2+2\sqrt{\gamma_1})} & -\sqrt{\gamma_1}\\ -\sqrt{\gamma_1} & \sqrt{\gamma_2+2\sqrt{\gamma_1}}\end{bmatrix},\\
\mathbf{Q}_{11}(\theta)&\equiv\mathbf{0},\qquad \mathbf{R}_{11}(\xi,\theta)\equiv\mathbf{0}\,.
\end{aligned} \tag{29}$$

Then, to obtain $\mathbf{P}_{12},\mathbf{Q}_{12}(\theta),\mathbf{Q}_{21}(\theta)$ we need to solve

$$
\begin{aligned}
&\hat{\mathbf{A}}_0\mathbf{P}_{12} + \tau\mathbf{P}_{12}\mathbf{A}_0 + \tau\mathbf{P}_{11}\mathbf{A}_1 + \mathbf{Q}_{12}(0) + \mathbf{Q}_{21}^{\mathrm{T}}(0) = \mathbf{0}\,,\\
&\partial_\theta\mathbf{Q}_{12}(\theta) = \hat{\mathbf{A}}_0\mathbf{Q}_{12}(\theta) + \mathbf{R}_{12}(0,\theta)\,,\\
&\partial_\theta\mathbf{Q}_{21}(\theta) = \big(\tau\mathbf{A}_0^{\mathrm{T}} - \tau^2\mathbf{P}_{12}^{\mathrm{T}}\mathbf{D}_1\mathbf{D}_1^{\mathrm{T}}\big)\mathbf{Q}_{11}(\theta) + \tau\mathbf{A}_0^{\mathrm{T}}\mathbf{Q}_{21}(\theta)\\
&\qquad + \mathbf{R}_{12}^{\mathrm{T}}(\theta,0)\,,\\
&(\partial_\xi + \partial_\theta)\mathbf{R}_{12}(\xi,\theta) = -\tau^2\mathbf{Q}_{11}^{\mathrm{T}}(\xi)\mathbf{D}\mathbf{D}^{\mathrm{T}}\mathbf{Q}_{12}(\theta)\,,
\end{aligned}
\tag{30}
$$

with boundary conditions

$$
\begin{aligned}
&\mathbf{Q}_{12}(-1) = \tau\mathbf{P}_{12}\mathbf{B}_0\,, \quad \mathbf{Q}_{21}(-1) = \mathbf{0}\,,\\
&\mathbf{R}_{12}(-1,\theta) = \mathbf{0}\,, \qquad \mathbf{R}_{12}(\theta,-1) = \tau\mathbf{Q}_{21}^{\mathrm{T}}(\theta)\mathbf{B}_0\,.
\end{aligned}
\tag{31}
$$

Then (30,31) give the solution

$$
\mathbf{Q}_{21}(\theta) \equiv \mathbf{0}, \qquad \mathbf{R}_{12}(\xi,\theta) \equiv \mathbf{0}\,, \tag{32}
$$

while the equations for $\mathbf{Q}_{12}(\theta)$ simplify to

$$
\partial_\theta\mathbf{Q}_{12}(\theta) = \hat{\mathbf{A}}_0\mathbf{Q}_{12}(\theta), \qquad \mathbf{Q}_{12}(-1) = \tau\mathbf{P}_{12}\mathbf{B}_0\,,
$$

yielding the solution

$$
\mathbf{Q}_{12}(\theta) = \tau\mathrm{e}^{\hat{\mathbf{A}}_0(\theta+1)}\mathbf{P}_{12}\mathbf{B}_0\,. \tag{33}
$$

Finally, the equation for $\mathbf{P}_{12}$ simplifies to

$$
\hat{\mathbf{A}}_0\mathbf{P}_{12} + \tau\mathbf{P}_{12}\mathbf{A}_0 + \tau\mathbf{P}_{11}\mathbf{A}_1 + \tau\mathrm{e}^{\hat{\mathbf{A}}_0}\mathbf{P}_{12}\mathbf{B}_0 = \mathbf{0}\,,
$$

yielding the solution

$$
\mathrm{vec}(\mathbf{P}_{12}) = \mathbf{M}_0\mathrm{vec}(\mathbf{P}_{11})\,. \tag{34}
$$

where $\mathrm{vec}(\cdot)$ gives a column vector by stacking the columns of the matrix on the top of each other and

$$
\mathbf{M}_0 = -\,\mathbf{L}^{-1}(\mathbf{A}_1^{\mathrm{T}} \otimes \mathbf{I})\,, \tag{35}
$$

where

$$
\mathbf{L} = \frac{1}{\tau}\mathbf{I} \otimes \hat{\mathbf{A}}_0 + \mathbf{A}_0^{\mathrm{T}} \otimes \mathbf{I} + \mathbf{B}_0^{\mathrm{T}} \otimes \mathrm{e}^{\hat{\mathbf{A}}_0}\,. \tag{36}
$$

For $\mathbf{P}_{1i}, \mathbf{Q}_{1i}(\theta)$, $i = 3, \cdots, n$, (22,23,24) yield

$$
\begin{aligned}
&\hat{\mathbf{A}}_0\mathbf{P}_{1i} + \tau\mathbf{P}_{1i}\mathbf{A}_0 + \tau\mathbf{P}_{1(i-1)}\mathbf{A}_1 + \mathbf{Q}_{1i}(0) + \mathbf{Q}_{i1}^{\mathrm{T}}(0) = \mathbf{0}\,,\\
&\partial_\theta\mathbf{Q}_{1i}(\theta) = \hat{\mathbf{A}}_0\mathbf{Q}_{1i}(\theta) + \mathbf{R}_{1i}(0,\theta)\,,\\
&\partial_\theta\mathbf{Q}_{i1}(\theta) = \mathbf{A}_0^{\mathrm{T}}\mathbf{Q}_{i1}(\theta) + \mathbf{A}_1^{\mathrm{T}}\mathbf{Q}_{(i-1)1}(\theta) + \mathbf{R}_{1i}^{\mathrm{T}}(\theta,0)\\
&\qquad - \mathbf{P}_{1i}^{\mathrm{T}}\mathbf{D}_1\mathbf{D}_1^{\mathrm{T}}\mathbf{Q}_{11}(\theta)\,,\\
&(\partial_\xi + \partial_\theta)\mathbf{R}_{1i}(\xi,\theta) = -\tau^2\mathbf{Q}_{11}^{\mathrm{T}}(\xi)\mathbf{D}\mathbf{D}^{\mathrm{T}}\mathbf{Q}_{1i}(\theta)\,,
\end{aligned}
\tag{37}
$$

with boundary conditions

$$
\begin{aligned}
&\mathbf{Q}_{1i}(-1) = \tau(\mathbf{P}_{1i}\mathbf{B}_0 + \mathbf{P}_{1(i-1)}\mathbf{B}_1)\,,\\
&\mathbf{Q}_{i1}(-1) = \mathbf{0},\\
&\mathbf{R}_{1i}(\theta,-1) = \tau\big(\mathbf{Q}_{i1}^{\mathrm{T}}(\theta)\mathbf{B}_0 + \mathbf{Q}_{(i-1)1}^{\mathrm{T}}(\theta)\mathbf{B}_1\big)\,,\\
&\mathbf{R}_{1i}(-1,\theta) = \mathbf{0}\,.
\end{aligned}
\tag{38}
$$

Following the steps above, (37,38) yield

$$
\mathbf{Q}_{i1}(\theta) \equiv \mathbf{0}, \qquad \mathbf{R}_{1i}(\xi,\theta) \equiv \mathbf{0}\,, \tag{39}
$$

and

$$
\mathbf{Q}_{1i}(\theta) = \tau\mathrm{e}^{\hat{\mathbf{A}}_0(\theta+1)}\big(\mathbf{P}_{1i}\mathbf{B}_0 + \mathbf{P}_{1(i-1)}\mathbf{B}_1\big)\,, \tag{40}
$$

for $i = 3, \ldots, n$, while $\mathbf{P}_{1i}$ is given by

$$
\mathrm{vec}(\mathbf{P}_{1i}) = (\mathbf{M}_1)^{i-2}\mathbf{M}_0\mathrm{vec}(\mathbf{P}_{11})\,, \tag{41}
$$

where

$$
\mathbf{M}_1 = -\,\mathbf{L}^{-1}(\mathbf{A}_1^{\mathrm{T}} \otimes \mathbf{I} + \mathbf{B}_1^{\mathrm{T}} \otimes \mathrm{e}^{\hat{\mathbf{A}}_0})\,, \tag{42}
$$

and $\mathbf{L}$ is given in (36).

Note that we can rewrite (29,33,40) in the compact form

$$
\mathbf{Q}_{1i}(\theta) = \mathrm{e}^{\hat{\mathbf{A}}_0(\theta+1)}\hat{\mathbf{Q}}_{1i}\,, \tag{43}
$$

where

$$
\hat{\mathbf{Q}}_{1i} = \begin{cases} \mathbf{0}, & i = 1\,,\\ \tau\mathbf{P}_{12}\mathbf{B}_0, & i = 2\,,\\ \tau\big(\mathbf{P}_{1i}\mathbf{B}_0 + \mathbf{P}_{1(i-1)}\mathbf{B}_1\big), & i \geq 3\,. \end{cases} \tag{44}
$$

3.2 Constructing the CCC controller

Denote

$$
\mathbf{P}_{1i} = -\begin{bmatrix} \times & \times \\ a_i & b_i \end{bmatrix}, \quad \mathbf{Q}_{1i}(\theta) = -\begin{bmatrix} \times & \times \\ f_i(\theta) & g_i(\theta) \end{bmatrix}, \tag{45}
$$

where

$$
\begin{aligned}
f_i(\theta) &= (a_{i0} + a_{i1}(\theta+1))\mathrm{e}^{\lambda_1(\theta+1)} + a_{i2}\mathrm{e}^{\lambda_2(\theta+1)}\,,\\
g_i(\theta) &= (b_{i0} + b_{i1}(\theta+1))\mathrm{e}^{\lambda_1(\theta+1)} + b_{i2}\mathrm{e}^{\lambda_2(\theta+1)}\,,
\end{aligned}
\tag{46}
$$

and λ_1, λ_2 are the eigenvalues of $\hat{\mathbf{A}}_0$. The expressions for $a_{i0}, a_{i1}, a_{i2}, b_{i0}, b_{i1}, b_{i2}$ are given in Appendix B.

With the optimized controller (25,45,46), the dynamics of the vehicle string (in rescaled time) is given by the DDE

$$
\begin{aligned}
&\dot{\tilde{h}}_1(t) = \tau\big(\tilde{v}_2(t) - \tilde{v}_1(t)\big)\,,\\
&\dot{\tilde{v}}_1(t) = \tau^2\sum_{i=1}^{n}\Big(a_i\tilde{h}_i(t) + b_i\tilde{v}_i(t)\\
&\qquad + \int_{-1}^{0}\big(f_i(\theta)\tilde{h}_i(t+\theta) + g_i(\theta)\tilde{v}_i(t+\theta)\big)\mathrm{d}\theta\Big)\,,\\
&\dot{\tilde{h}}_i(t) = \tau\big(\tilde{v}_{i+1}(t) - \tilde{v}_i(t)\big)\,,\\
&\dot{\tilde{v}}_i(t) = \tau\big(\alpha f^*\tilde{h}_i(t-1) - (\alpha+\beta)\tilde{v}_i(t-1) + \beta\tilde{v}_{i+1}(t-1)\big)\,,
\end{aligned}
\tag{47}
$$

for $i = 2, \ldots, n$, cf. (5).

The optimized gains a_i, b_i of the CCC controller are related through (41). We found that the eigenvalues of $\mathbf{M}_1$ (cf. (42)) are inside the unit circle for realistic values of weighting factors γ_1, γ_2, human gains α, β, and driver reaction time τ. Thus (41) is a contracting map, and consequently, a_i, b_i decay with the vehicle index $i = 2, \ldots, n$. As an example, we consider $\gamma_1 = 1\,[1/\mathrm{s}^2]$, $\gamma_2 = 4\,[1/\mathrm{s}]$, $\alpha = 0.4\,[1/\mathrm{s}], \beta = 0.5\,[1/\mathrm{s}]$ and $\tau = 0.4\,[\mathrm{s}]$. In this case, $\mathbf{M}_1$ has two zero eigenvalues and two non-zero eigenvalues 0.55 and 0.13.

Fig. 2 shows the exponential decay of a_i and b_i in a $(5+1)$ vehicle chain (red circles) and a $(10+1)$ vehicle chain (blue crosses) using the aforementioned parameter values. The exact match between the red circles and the blue crosses for vehicles 2 to 5 demonstrate that the existing optimized gains are not changed by adding feedback terms on vehicles farther away. This corresponds to the fact that the gains a_1, b_1 are not influenced by the connectivity structure (cf. (29) and (45)), and a_i, b_i are calculated recursively using (34) and (41). For the parameters considered above, we have the gains $a_1 \approx 2.50\,[1/\mathrm{s}]$, $b_1 \approx -6.12\,[1/\mathrm{s}]$.

Note that $\mathbf{Q}_{1i}(\theta)$ contains the same distribution matrix $\mathrm{e}^{\hat{\mathbf{A}}_0(\theta+1)}$ for all i (cf. (43)), where $\hat{\mathbf{A}}_0$ (cf. (28)) depends on the driver reaction time τ and weighting factors γ_1 and γ_2 through $\mathbf{P}_{11}$ (cf. (29)). The distribution functions $f_i(\theta), g_i(\theta)$ are linear combinations of the elements of $\mathrm{e}^{\hat{\mathbf{A}}_0(\theta+1)}$ (cf. (B.3) in Appendix B). We plot $f_i(\theta)$ and $g_i(\theta)$ for $i = 2, \ldots, 5$ in Fig. 3 using the same parameters as in Fig. 2. Note that $f_1(\theta) \equiv 0$ and $g_1(\theta) \equiv 0$, i.e., the

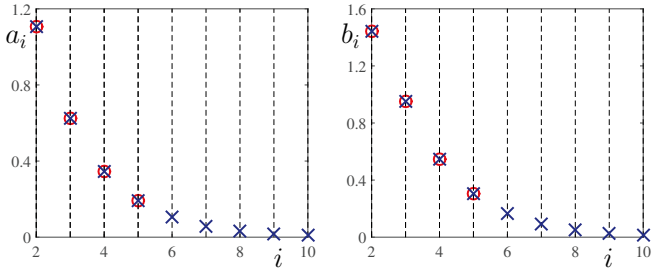

Fig. 2. The optimized headway and velocity gains $a_i, b_i, i = 2, \ldots, n$ of the CCC vehicle for a string of $(n+1)$ vehicles. Red circles correspond to $n = 5$ while blue crosses are for $n = 10$. The human gains are set to $\alpha = 0.4\,[1/\mathrm{s}], \beta = 0.5\,[1/\mathrm{s}]$, and the driver reaction time is $\tau = 0.4\,[\mathrm{s}]$. The weighting factors are $\gamma_1 = 1\,[1/\mathrm{s}^2]$, $\gamma_2 = 4\,[1/\mathrm{s}]$.

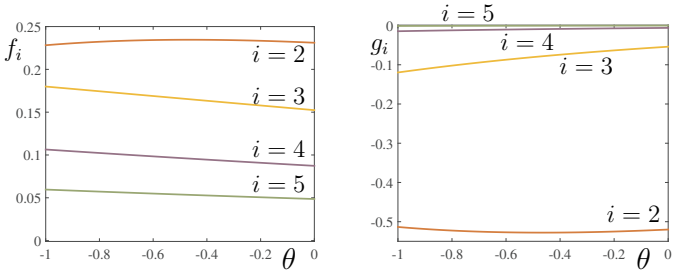

Fig. 3. The distribution functions $f_i(\theta), g_i(\theta)$ for a $(5+1)$-vehicle system with the same human parameters as in Fig. 2. The blue, red, yellow, purple, and green curves correspond to $i = 1, \ldots, 5$, respectively.

optimized controller does not use delayed information of CCC vehicle itself. While for each $i = 2, \ldots, n$, $f_i(\theta)$ and $g_i(\theta)$ may increase or decrease with $\theta \in [-1, 0]$, in general the magnitude of $f_i(\theta)$ and $g_i(\theta)$ decays with i.

Since the relation between LQR and pole assignment can be extended to the delayed cases, the controller derived from LQR places the eigenvalues of the system in the left half of the complex plane, i.e., guarantees stability of the equilibrium.

3.3 Simulations

In this section, we test the performance of the proposed CCC controller using numerical simulations. We consider a vehicle string with $5 + 1$ vehicles with initial condition $X(t) \equiv 0, t \in [-1, 0]$ and a triangular velocity disturbance signal

$$\tilde{v}_{n+1}(t) = \begin{cases} 0 & -1 \le t \le 0\,, \\ -t & 0 < t \le 8\,, \\ t - 16 & 8 < t \le 24\,, \\ -t + 32 & 24 < t \le 32\,, \\ 0 & t > 32\,, \end{cases} \tag{48}$$

see the dashed curve in Fig. 4(b). In Fig. 4, we plot the corresponding headway and velocity perturbations for the system (47) with the same parameter as in Fig. 2. The velocity and headway of the CCC vehicle (red thick curves) converge to the equilibrium. We also show the case when the CCC vehicle loses connectivity with vehicles $3, 4, 5$ (black thick curves), i.e., $a_i = 0, b_i = 0$, $f_i(\theta) \equiv 0, g_i(\theta) \equiv 0$, for $i = 3, 4, 5$ in (47). In this case, the CCC vehicle only relies on the link from vehicle 2. Although its headway and velocity perturbations still converge to zero, demonstrating the robustness of the proposed controller, the black curves have larger amplitude than the red curves. This shows the potential benefits of having feedback terms from multiple vehicles ahead.

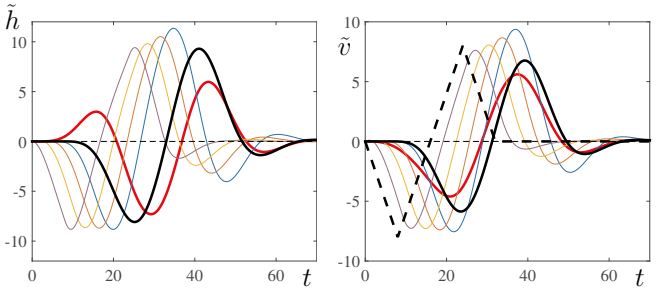

Fig. 4. Headway and velocity fluctuations of a $(5+1)$-car vehicle string with the same parameters as in Fig. 2. The thick red curves correspond to the CCC vehicle using information from vehicles $2-5$, while the thick black curves are when the CCC vehicle only uses information from vehicle 2. The thin curves correspond to the non-CCC vehicles. The black dashed curve is the disturbance profile (48).

Notice that the amplitude of CCC vehicle's velocity response is smaller than the disturbance input $\tilde{v}_{n+1}(t)$, i.e., the velocity perturbation is attenuated as it reaches the tail vehicle. This property is called string stability, and is highly desirable to avoid amplification of congestion waves; see Seiler et al. (2004), Orosz et al. (2010). Although string stability is not considered in this paper, this property can be achieved by choosing appropriate weighting factors γ_1, γ_2.

4. CONCLUSION

In this paper, we proposed a connected cruise control design where the connectivity structure was optimized using linear quadratic regulation while considering driver reaction time delay. We found that the feedback gains on signals from nearby vehicles were not influenced by dynamics of vehicles farther downstream, and the gains decreased exponentially with the number of cars between the CCC vehicle and the signaling vehicle. The performance of the CCC controller was tested using numerical simulation. The proposed control algorithm can be extended to vehicle systems with heterogeneous driver parameters, and multiple CCC vehicles. When considering non-zero time delay in the wireless communication, the closed-loop system also contains an actuator delay; see Kristic (2009). A detailed discussion on the choice of the design parameters γ_1, γ_2 to ensure plant and string stability will be considered in the future. Also, nonlinear CCC algorithms and partial knowledge about the motion of non-CCC vehicles will be investigated.

ACKNOWLEDGEMENTS

This work was supported by the National Science Foundation (Award Number 1351456).

REFERENCES

Ge, J.I. and Orosz, G. (2014a). Dynamics of connected vehicle systems with delayed acceleration feedback. *Transportation Research Part C*, 46, 46–64.

Ge, J.I. and Orosz, G. (2014b). Optimal control of connected vehicle systems. In *Conference on Decision and Control, IEEE*, 4107–4112.

Kolmanovskii, V. and Myshkis, A. (1992). *Applied Theory of Functional Differential Equations*. Kluwer Academic Publisher.

Kristic, M. (2009). *Delay Compensation for Nonlinear, Adaptive, and PDE Systems*. Birkhauser.

Orosz, G. (2014). Connected cruise control: modeling, delay effects, and nonlinear behavior. *Vehicle System Dynamics*, submitted.

Orosz, G., Wilson, R.E., and Stépán, G. (2010). Traffic jams: dynamics and control. *Philosophical Transactions of the Royal Society A*, 368(1928), 4455–4479.

Ploeg, J., Shukla, D., van de Wouw, N., and Nijmeijer, H. (2014). Controller synthesis for string stability of vehicle platoons. *IEEE Transactions on Intelligent Transportation Systems*, 15(2), 845–865.

Qin, W.B., Gomez, M.M., and Orosz, G. (2014). Stability analysis of connected cruise control with stochastic delays. In *Proceedings of American Control Conference*, 4624–4629. IEEE.

Ross, D. and Flugge-Lotz, I. (1969). An optimal control problem for systems with differential-difference equation dynamics. *SIAM Journal on Control*, 7(4), 609–623.

Seiler, P., Pant, A., and Hedrick, K. (2004). Disturbance propagation in vehicle strings. *IEEE Transactions on Automatic Control*, 49(10), 1835–1842.

Wang, M., Daamen, W., Hoogendoorn, S.P., and van Arem, B. (2014). Rolling horizon control framework for driver assistance systems. part II: Cooperative sensing and cooperative control. *Transportation Research Part C*, 40, 290–311.

Zhang, L. and Orosz, G. (2015). Motif-based analysis of connected vehicle systems: delay effects and stability. *IEEE Transactions on Intelligent Transportation Systems*, submitted.

Appendix A. THE SOLUTION OF LQR PROBLEM WITH DELAY

Here we present a detailed solution to the LQR problem with time delay. Since (11,12) is constructed to include disturbance $\phi(t)$ in the LQR format, and the optimal controller (18) is given using partitioned matrices (17). We write (15,16) into four groups, where $\mathbf{P}_1(t)$, $\mathbf{Q}_1(t,\theta)$, $\mathbf{R}_1(t,\xi,\theta)$ are independent from the disturbance and can be solved using only the coefficient matrices $\mathbf{A},\mathbf{B},\mathbf{D}$ and the weighting factor $\mathbf{\Gamma}$. That is, for the first group we obtain the PDE

$$\begin{aligned}
-\dot{\mathbf{P}}_1(t) &= \tau\mathbf{A}^{\mathrm{T}}\mathbf{P}_1(t) + \tau\mathbf{P}_1(t)\mathbf{A} + \mathbf{Q}_1(t,0) + \mathbf{Q}_1^{\mathrm{T}}(t,0) \\
&\quad + \mathbf{\Gamma} - \tau^2\mathbf{P}_1(t)\mathbf{D}\mathbf{D}^{\mathrm{T}}\mathbf{P}_1(t)\,, \\
(\partial_\theta - \partial_t)\mathbf{Q}_1(t,\theta) &= \big(\tau\mathbf{A}^{\mathrm{T}} - \tau^2\mathbf{P}_1(t)\mathbf{D}\mathbf{D}^{\mathrm{T}}\big)\mathbf{Q}_1(t,\theta) \\
&\quad + \mathbf{R}_1(t,0,\theta)\,, \\
(\partial_\xi + \partial_\theta - \partial_t)\mathbf{R}_1(t,\xi,\theta) &= -\tau^2\mathbf{Q}_1^{\mathrm{T}}(t,\xi)\mathbf{D}\mathbf{D}^{\mathrm{T}}\mathbf{Q}_1(t,\theta)\,,
\end{aligned} \tag{A.1}$$

with boundary conditions

$$\begin{aligned}
&\mathbf{P}_1(t_{\mathrm{f}}) = \mathbf{0}\,, \\
&\mathbf{Q}_1(t_{\mathrm{f}},\theta) = \mathbf{0}\,, \qquad \mathbf{Q}_1(t,-1) = \tau\mathbf{P}_1(t)\mathbf{B}\,, \\
&\mathbf{R}_1(t_{\mathrm{f}},\xi,\theta) = \mathbf{0}\,, \qquad \mathbf{R}_1(t,-1,\theta) = \tau\mathbf{B}^{\mathrm{T}}\mathbf{Q}_1(t,\theta)\,.
\end{aligned} \tag{A.2}$$

Using $\mathbf{P}_1(t)$ and $\mathbf{Q}_1(t,\theta)$ obtained from (A.1,A.2), we can calculate $\mathbf{Q}_2(t,\theta)$ and $\mathbf{R}_2(t,\xi,\theta)$ by solving

$$\begin{aligned}
(\partial_\theta - \partial_t)\mathbf{Q}_2(t,\theta) &= \big(\tau\mathbf{A}^{\mathrm{T}} - \tau^2\mathbf{P}_1(t)\mathbf{D}\mathbf{D}^{\mathrm{T}}\big)\mathbf{Q}_2(t,\theta) \\
&\quad + \mathbf{R}_2(t,0,\theta)\,, \\
(\partial_t - \partial_\xi - \partial_\theta)\mathbf{R}_2(t,\xi,\theta) &= \tau^2\mathbf{Q}_1^{\mathrm{T}}(t,\xi)\mathbf{D}\mathbf{D}^{\mathrm{T}}\mathbf{Q}_2(t,\theta)\,,
\end{aligned} \tag{A.3}$$

with boundary conditions

$$\begin{aligned}
&\mathbf{Q}_2(t_{\mathrm{f}},\theta) = \mathbf{0}\,, \qquad \mathbf{R}_2(t_{\mathrm{f}},\xi,\theta) = \mathbf{0}\,, \\
&\mathbf{Q}_2(t,-1) = \mathbf{0}\,, \qquad \mathbf{R}_2(t,-1,\theta) = \tau\mathbf{B}^{\mathrm{T}}\mathbf{Q}_2(t,\theta)\,.
\end{aligned} \tag{A.4}$$

Note that the disturbance $\phi(t)$ does not appear in (A.3) either. As a matter of fact, (A.3,A.4) result in $\mathbf{Q}_2(t,\theta)\equiv\mathbf{0}$ and $\mathbf{R}_2(t,\xi,\theta)\equiv\mathbf{0}$.

The dynamics of $\mathbf{P}_2(t)$ and $\mathbf{Q}_3(t,\theta)$ are driven by the disturbance $\phi(t)$:

$$\begin{aligned}
-\dot{\mathbf{P}}_2(t) &= \big(\tau\mathbf{A}^{\mathrm{T}} - \tau^2\mathbf{P}_1(t)\mathbf{D}\mathbf{D}^{\mathrm{T}}\big)\mathbf{P}_2(t) + \mathbf{P}_1(t)\phi(t) \\
&\quad + \mathbf{Q}_2(t,0) + \mathbf{Q}_3^{\mathrm{T}}(t,0)\,, \\
(\partial_\theta - \partial_t)\mathbf{Q}_3(t,\theta) &= \big(\phi^{\mathrm{T}}(t) - \tau^2\mathbf{P}_2^{\mathrm{T}}(t)\mathbf{D}\mathbf{D}^{\mathrm{T}}\big)\mathbf{Q}_3(t,\theta) \\
&\quad + \mathbf{R}_2^{\mathrm{T}}(t,\theta,0)\,,
\end{aligned} \tag{A.5}$$

with boundary conditions

$$\mathbf{P}_2(t_{\mathrm{f}}) = \mathbf{0}\,, \qquad \mathbf{Q}_3(t_{\mathrm{f}},\theta) = \mathbf{0}\,, \qquad \mathbf{Q}_3(t,-1) = \tau\mathbf{P}_2^{\mathrm{T}}(t)\mathbf{B}\,. \tag{A.6}$$

Although $\mathbf{P}_4(t)$, $\mathbf{Q}_4(t,\theta)$, $\mathbf{R}_4(t,\xi,\theta)$ do not appear in the optimal control (18), they appear in the minimal cost function, and are given by the PDE

$$\begin{aligned}
-\dot{\mathbf{P}}_4(t) &= \tau\phi^{\mathrm{T}}(t)\mathbf{P}_2(t) + \tau\mathbf{P}_3(t)\phi(t) + \mathbf{Q}_4(t,0) + \mathbf{Q}_4^{\mathrm{T}}(t,0) \\
&\quad - \tau^2\mathbf{P}_3(t)\mathbf{D}\mathbf{D}^{\mathrm{T}}\mathbf{P}_2(t)\,, \\
(\partial_\theta - \partial_t)\mathbf{Q}_4(t,\theta) &= \big(\tau\phi^{\mathrm{T}}(t) - \tau^2\mathbf{P}_3(t)\mathbf{D}\mathbf{D}^{\mathrm{T}}\big)\mathbf{Q}_4(t,\theta) \\
&\quad + \mathbf{R}_4(t,0,\theta)\,, \\
(\partial_\xi + \partial_\theta - \partial_t)\mathbf{R}_4(t,\xi,\theta) &= -\tau^2\mathbf{Q}_2^{\mathrm{T}}(t,\xi)\mathbf{D}\mathbf{D}^{\mathrm{T}}\mathbf{Q}_2(t,\theta)\,,
\end{aligned} \tag{A.7}$$

with boundary conditions

$$\begin{aligned}
&\mathbf{P}_4(t_{\mathrm{f}}) = \mathbf{0}\,, \\
&\mathbf{Q}_4(t_{\mathrm{f}},\theta) = \mathbf{0}\,, \qquad \mathbf{Q}_4(t,-1) = \mathbf{0}\,, \\
&\mathbf{R}_4(t_{\mathrm{f}},\xi,\theta) = \mathbf{0}\,, \qquad \mathbf{R}_4(t,-1,\theta) = \mathbf{0}\,.
\end{aligned} \tag{A.8}$$

Appendix B. THE DISTRIBUTION FUNCTIONS

Since $\mathbf{Q}_{1i}(\theta)$ given in (43,44) contains $\mathrm{e}^{\hat{\mathbf{A}}_0(\theta+1)}$, we write

$$\mathrm{e}^{\hat{\mathbf{A}}_0(\theta+1)} = \mathbf{K}\mathrm{e}^{\mathbf{J}_0(\theta+1)}\mathbf{K}^{-1}\,, \tag{B.1}$$

where $\mathbf{J}_0$ is the Jordan form of $\hat{\mathbf{A}}_0$, and $\mathbf{K}$ is the corresponding transformation matrix. Denote the eigenvalues of $\hat{\mathbf{A}}_0$ as λ_1,λ_2, then

$$\begin{aligned}
\mathrm{e}^{\hat{\mathbf{A}}_0(\theta+1)} &= \left(\begin{bmatrix}\tilde{a}_{11} & \tilde{a}_{12}\\ \tilde{a}_{21} & \tilde{a}_{22}\end{bmatrix} + (\theta+1)\begin{bmatrix}\tilde{b}_{11} & \tilde{b}_{12}\\ \tilde{b}_{21} & \tilde{b}_{22}\end{bmatrix}\right)\mathrm{e}^{\lambda_1(\theta+1)} \\
&\quad + \begin{bmatrix}\tilde{c}_{11} & \tilde{c}_{12}\\ \tilde{c}_{21} & \tilde{c}_{22}\end{bmatrix}\mathrm{e}^{\lambda_2(\theta+1)}\,,
\end{aligned} \tag{B.2}$$

where $\tilde{b}_{ij}\neq 0$ when $\mathbf{K}$ contains generalized eigenvectors. Substituting (B.2) into (43,44), we obtain (45,46) with

$$\begin{aligned}
&[a_{i0}\,b_{i0}] = [\tilde{a}_{21}\,\tilde{a}_{22}]\hat{\mathbf{Q}}_{1i}, \qquad [a_{i1}\,b_{i1}] = [\tilde{b}_{21}\,\tilde{b}_{22}]\hat{\mathbf{Q}}_{1i}, \\
&[a_{i2}\,b_{i2}] = [\tilde{c}_{21}\,\tilde{c}_{22}]\hat{\mathbf{Q}}_{1i}\,.
\end{aligned} \tag{B.3}$$